One-Cell Doubling Evaluation by Living Arrays of Yeast, ODELAY!

Thurston Herricks,* David J. Dilworth,* Fred D. Mast,*,† Song Li,* Jennifer J. Smith,* Alexander V. Ratushny,*,† and John D. Aitchison*,†,1
*Institute for Systems Biology and †Center for Infectious Disease Research, Seattle, Washington 98109
ORCID ID: 0000-0002-2177-6647 (F.D.M.)

ABSTRACT Cell growth is a complex phenotype widely used in systems biology to gauge the impact of genetic and environmental perturbations. Due to the magnitude of genome-wide studies, resolution is often sacrificed in favor of throughput, creating a demand for scalable, time-resolved, quantitative methods of growth assessment. We present ODELAY (One-cell Doubling Evaluation by Living Arrays of Yeast), an automated and scalable growth analysis platform. High measurement density and single-cell resolution provide a powerful tool for large-scale multiparameter growth analysis based on the modeling of microcolony expansion on solid media. Pioneered in yeast but applicable to other colony forming organisms, ODELAY extracts the three key growth parameters (lag time, doubling time, and carrying capacity) that define microcolony expansion from single cells, simultaneously permitting the assessment of population heterogeneity. The utility of ODELAY is illustrated using yeast mutants, revealing a spectrum of phenotypes arising from single and combinatorial growth parameter perturbations.

KEYWORDS
growth rate
lag time
carrying capacity
fitness
assessment
yeast

Growth is a well-established, sensitive metric of cellular fitness that is widely used to interrogate genetic and environmental interactions. The most basic models of microorganism population expansion over time consist of three distinct phases: lag phase, log phase, and stationary phase (Monod 1949). Each phase is defined by a specific parameter that uniquely contributes to overall fitness. Lag phase, defined by lag time, is the period after initial inoculation wherein little to no growth is observed. Following acclimation, the population enters log phase and expands exponentially at a constant, maximal rate defined by the doubling time. Finally, a rapid cessation of growth is observed as the population enters stationary phase, having reached its maximum attainable level defined by the carrying capacity. By virtue of its linear nature during exponential growth, the log plot of population number *vs.* time has classically been employed to extract the three key growth parameters. Lag time is the period up to the attainment of linearity of the log-plot, doubling time is inversely proportional to the slope of the linear region of the log-plot, and carrying capacity is the maximum population size when the slope of the log plot approaches zero.

In light of its relatively well-understood cell biology and genetic tractability, baker's yeast, *Saccharomyces cerevisiae*, is a model organism commonly exploited to elucidate genetic and environmental interactions on a genome-wide scale. Many methods of assessing yeast strain growth characteristics have been described. One of the oldest and most common methods to quantify yeast growth is to measure the increase of turbidity in liquid culture over time (Peskett 1927) as now routinely measured by absorbance of 600 nm light (OD600). It was also the first to be automated (Jørgensen and Schulz 1985). This robust measurement has been parallelized in 96-well and 200-well formats to evaluate the genome deletion library (Warringer *et al.* 2008; Yoshikawa *et al.* 2009). Variations in liquid culture growth assays have been extended to incorporate flow cytometry or sequencing to measure competitive growth of genetically modified mixed cultures on a genome-wide scale (Winzeler *et al.* 1999; Tucker and Fields 2004; Deutschbauer *et al.* 2005; Breslow *et al.* 2008; Kortmann *et al.* 2009; Murakami and Kaeberlein 2009; Bryan *et al.* 2010; Godin *et al.* 2010; Sun *et al.* 2010). Heterogeneity of yeast growth rates has been observed with time-lapse microscopy of precipitated liquid cultures (Levy *et al.* 2012). However, dynamic range limitations associated with many liquid culture methods render them unable to assess all three growth parameters within a single

doi: 10.1534/g3.116.037044
Manuscript received August 22, 2016; accepted for publication November 10, 2016; published Early Online November 16, 2016.

Supplemental material is available online at www.g3journal.org/lookup/suppl/doi:10.1534/g3.116.037044/-/DC1.
[1]Corresponding author: Institute for Systems Biology, 401 Terry Ave. N., Seattle, WA 98109. E-mail: john.aitchison@systemsbiology.org

experimental run; thus, analyses are often restricted to only one growth parameter, most commonly doubling time. Furthermore, difficulties associated with maintaining low volume yeast cultures in suspension at high densities limit the throughput of many liquid growth analysis techniques (Kortmann *et al.* 2009).

The shortcomings inherent to yeast liquid culture assays have made it commonplace to employ cell spotting as a proxy for strain growth. Common cell spotting assays range from colony pinning assays, in which a pin is used to deliver a patch of cells onto the surface of solid agar media to serial dilution spotting analysis, wherein single colonies are obtained (Memarian *et al.* 2007; Shah *et al.* 2007; Lawless *et al.* 2010). While these methods are universally accepted, there are significant caveats to their use. Foremost, most large-scale colony pinning fitness assays are traditionally assessed from a single time point (Collins *et al.* 2006; Baryshnikova *et al.* 2010; Costanzo *et al.* 2010, 2016). The lack of temporal resolution makes it impossible to deconvolve the different stages of population growth and, therefore, apparent differences in fitness cannot be attributed to the classically defined growth parameters of doubling time, lag time, and carrying capacity.

More recently, flatbed scanners and single-lens reflex (SLR) cameras have been used to periodically image pinned arrays of growing colonies (Levin-Reisman *et al.* 2010; Bean *et al.* 2014; Zackrisson *et al.* 2016). While these methods allow for collection of growth parameters, the recorded images have a resolution of 20–30 μm (or greater) per pixel. This pixel size thus limits spatial resolution to distinguishing features greater than about 40–60 μm in dimension. Since yeast cells are 3–5 μm in size, flatbed scanners and SLR cameras with a macrolens can only resolve colonies containing in the order of hundreds to thousands of cells, which also prevents these methods from directly observing lag time. Corrections for growth artifacts arising from competition between adjacent colonies and variations in media composition must also be included in the data analysis pipeline. In the case of the widely used synthetic genetic array (SGA), epistatic miniarray profile (E-MAP), SCANlag, and Scan-o-matic methods, effects of some confounding factors are corrected by the latest generation of analytical tools; however, given that multiple data sets involving many query strains are required to normalize for batch effects (Baryshnikova *et al.* 2010), sensitivity is proportional to the scale of the study using these methods, which can limit their practical utility.

In this work, we present a platform capable of high-density measurements of lag times prior to the attainment of doubling times during exponential growth, and carrying capacities at stationary phase through time course microscopy-based imaging of microcolonies growing on solid media. Because each microcolony is seeded from one to a few cells and hundreds of microcolonies can be analyzed for each strain, population heterogeneity of the three growth parameters can be assessed on a strain-by-strain basis. Through increased sensitivity and the potential for growth parameter profiling, the enhanced resolution afforded by this novel method of multiparameter fitness assessment can facilitate the generation and/or refinement of gene–gene and gene–environment interaction networks for yeast and other colony forming organisms.

MATERIALS AND METHODS

Yeast strains and growth conditions

Unless otherwise specified, all experiments were performed at 30° temperature using rich growth media, YEPD [1% w/v yeast extract (BD), 2% w/v peptone (BD), and 2% w/v dextrose (BD)]. Galactose growth media contained 2% w/v galactose (Acros) in place of glucose and solid media contained 2% w/v agar (BD) for cell spotting assays or 1.0% w/v agarose (Invitrogen) for ODELAY analyses. *S. cerevisiae* strains used in this study are listed in Supplemental Material, Table S1. All strains have been previously described (Deutschbauer *et al.* 2005; Memarian *et al.* 2007).

ODELAY culture preparation

First, 220 μl yeast cultures were inoculated in 96-well flat bottom plates (Corning Costar) and grown overnight. Cultures were then diluted 1:11 and optical densities read using a Synergy H4 plate reader. Individual wells were then diluted to a density of 0.09 OD and the culture grown for 6 hr to ensure all strains were in exponential phase. The cultures were again measured using the plate reader and then diluted to 0.01 OD. The 96-well plate containing the prepared cultures was then sonicated for 30 sec in an ice-cold water ultrasonic bath to dissociate cell clusters.

ODELAY slide preparation and yeast array setup

It is noteworthy that the sensitivity of ODELAY makes the method sensitive to growth conditions and so reproducible slide preparation is important. Growth media was prepared as a 1:1:8 mixture of the following sterile stock solutions, respectively: 10 × YEP (10% w/v yeast extract and 20% w/v peptone), 20% w/v carbon source (glucose or galactose), and 1.33% w/v agarose in water. Typically, a 150 ml volume of 1.33% agarose stock was prepared, divided into 15 ml aliquots in 50 ml conical bottom tubes, and stored at 4° until use. Agarose aliquots with 2 ml 10 × YEP and 2 ml 20% carbon source were placed in rapidly boiling water for 20 min to completely melt the agarose gel. Water lost to evaporation was replaced by weighing the conical tube before and after boiling, yielding a final growth substrate containing 1% yeast extract, 2% peptone, 2% carbon source, and 1% agarose. The molten solution was poured into custom molds that formed 2 mm slabs of agar supported by 50 mm by 75 mm by 0.1 inch glass slides (Fisher Scientific). The apparatus was allowed to cool to room temperature and, after separation of the glass slides, the agar plates were equilibrated overnight in a humidified chamber at 4°. Careful separation of the glass slides was critical as any mechanical deformation of the agar altered the lag time and doubling time of cultures in the regions deformed. The following day, yeast cells in exponential liquid culture, diluted to an OD_{600} of ~0.01, were spotted onto agarose slabs using a Matrix Hydra DT fluidics robot (Thermo Scientific). Slides were air dried for ~3–5 min and then placed inside a microscope equipped with a humidified environmental chamber maintained at 30°. This yields approximately 300 single cells per 9 mm^2. Spotting at higher density leads to merging of colonies and fewer measurements overall. The stage was then leveled so that cells remained in focus across the entire 8 × 12 spotted array.

ODELAY image acquisition time course

Bright field images were captured using a Leica DMI6000 microscope (Leica) equipped with a 10 × objective. Images were recorded by a Hammamasu ORCA Flash 4.0 camera. The microscope stage movements and camera were controlled by a custom MATLAB graphical user interface using the Micromanager Core API version 1.4 (Edelstein *et al.* 2014). MATLAB scripts controlled the stage to predefined positions. A custom autofocus routine found focus at the center of each spot by maximizing the image's focus score utilizing the Laplacian variance function (Pertuz *et al.* 2013). After focus was found, a 3 × 3 tiled image was recorded that covered a 9 mm^2 area of the agar. Since the stage was leveled before image collection, the focus did not drift appreciably across the tiled images. These steps were repeated on each of the 96 spotted strains in either 30 min or 1 hr increments for 48 hr.

Automated ODELAY image analysis

Image acquisition and panorama stitching were performed using MATLAB scripts. Briefly, images were stitched using a method based on FFT phases (Preibisch *et al.* 2009). A threshold of the stitched images was calculated by taking histograms of a subdivided image and finding the maximum intensities of 100 regions within the subdivided images. This threshold was used to binarize images and colony area was quantified using MATLAB functions. The $\log_2$ of colony area was plotted *vs.* time and colony area fitted to a parameterized version of the Gompertz function (Gompertz 1825; Zwietering *et al.* 1990),

$$f(t) = a_0 + be^{-e^{\left[\frac{e\,v_{\max}}{b}\left(t_{lag}-t\right)+\log\left(\frac{3+\sqrt{5}}{2}\right)\right]}} \quad (1)$$

where a_o and b are parameters that represent the initial size and final saturation of the colonies; $v_{\max}$ maximum growth velocity, and t_{lag} colony lag time. Growth parameters were solved for directly. The *gompertzFit* routine calculates an initial estimate of the Gompertz function using a coarse grid optimization and then attempts to find a constrained minimum of the function at this initial estimate using the *fmincon* MATLAB function. In order to proceed to curve fitting, colonies must be matched at five or more time points through the monitored time course. In addition, colonies that do not exhibit at least a doubling in area are eliminated from curve fitting. This is achieved by only fitting data for which the maximum observed cross-sectional area of each tracked object is at least twofold greater than the object's measured cross-sectional area at the first time point. Doubling time (t_d) is calculated as follows:

$$t_d = \frac{\ln 2}{v_{\max}}, \quad (2)$$

where $v_{\max}$ is the point at which the growth rate, $f'(t)$, reaches maximum (achieved at $f''(t) = 0$). Lag time (t_{lag}) is defined as the time to reach maximum growth acceleration, a_{max}, where $f''(t)$ is greatest (achieved at the lower value of the two solutions to $f'''(t) = 0$). The carrying capacity (K), in pixel area, represents the cross-sectional area of the base of the modeled microcolony projected to stationary phase ($f(t)$ as $t \to \infty$) and is calculated as follows:

$$K = a + b \quad (3)$$

BioScreen doubling time determination

Automated optical density measurements of yeast cultures were obtained using a BioScreen C (Growth Curves USA) using the manufacturer's suggested protocols, with the exception that culture volume was reduced to 200 μl to prevent artifacts arising from liquid splashing onto the plate lid during maximal agitation. A starting OD_{600} of 0.05 was utilized in order to ensure that cultures were in exponential phase once they entered the empirically determined linear range of the instrument. Growth curves were fit using the *gompertzFitBioScreen* function, which is identical to the *gompertzFit* function except that it is optimized for the range of OD_{600} values obtained from the Bioscreen C instead of observed area.

Data availability

The authors state that all data necessary for confirming the conclusions presented in the article are represented fully within the article. Datasets and files to analyze them can be found at http://aitchisonlab.com/ODELAY.

RESULTS AND DISCUSSION

Development of an automated scalable solid-phase doubling time estimation platform

An ideal solid-phase, time-resolved, growth analysis platform would allow for high sample density and be amenable to automated data acquisition and processing. The optimized method, which we have termed ODELAY, is depicted schematically (Figure 1) and consists of four stages: spotting arrays of live yeast onto thin beds of growth substrate on a glass slide support (Figure 1A); periodic bright field image acquisition over a user-specified time course (Figure 1B); processing of raw bright field data to extract microcolony cross-sectional area data (Figure 1C); and postprocessing calculation of growth parameters for each individual microcolony within each spot (Figure 1D). ODELAY is applicable to a wide range of growth substrates and incubation temperatures and is highly scalable, as it can analyze between 10^5 and 10^6 individual microcolonies per experiment.

ODELAY consists of an automated pipeline that encompasses acquisition and processing of images, identification and measurement of microcolonies at each time point, matching of microcolonies through time, and extrapolation of growth parameters from growth curves. This current platform employs theoretical approximation of ODELAY growth curves using the Gompertz function as an unsupervised method to extract growth parameters (Gompertz 1825; Preibisch *et al.* 2009). All files required for execution of automated ODELAY analysis, as well as a demonstrative data set, are available as Supplemental Material (File S1 and File S2).

Determination of growth parameters by ODELAY

First, data are acquired, and then growth parameters of doubling time, lag time, and carrying capacity are determined by directly fitting a parameterized version of the Gompertz function (Equation 1). For data acquisition, the first time point would ideally be acquired immediately after spotting onto agar at the desired growth temperature, but for practical purposes, the starting time is when the cells are spotted at room temperature on the solid substrate. The plate is then transferred to an environmentally controlled chamber and growing colonies are tracked until they merge with their neighbors. The time required for colonies to merge is therefore related to the initial cell density and the ultimate carrying capacity of adjacent colonies. While many colonies merge before carrying capacities are observed, ODELAY will still estimate carrying capacity as long as a sufficient number of data points are collected after maximum growth velocity is achieved. This is a feature of the Gompertz function's symmetry about maximum growth velocity, which permits fair estimation of carrying capacity even when it is not directly measured. Note that caution should be exercised when examining phenotypes associated with increased carrying capacity because the Gompertz function may not accurately estimate all possible outcomes.

Comparison of ODELAY to established methods

We directly compared doubling times and lag times calculated by multiple ODELAY population measurements to liquid culture OD_{600} measurements made using the BioScreen C instrument for both fast and slow growing strains taken from the MATα yeast deletion library (Winzeler *et al.* 1999) (Figure 2A). Population doubling times and precision of this measurement across replicates were roughly comparable between the two platforms (Figure 2A). Measured

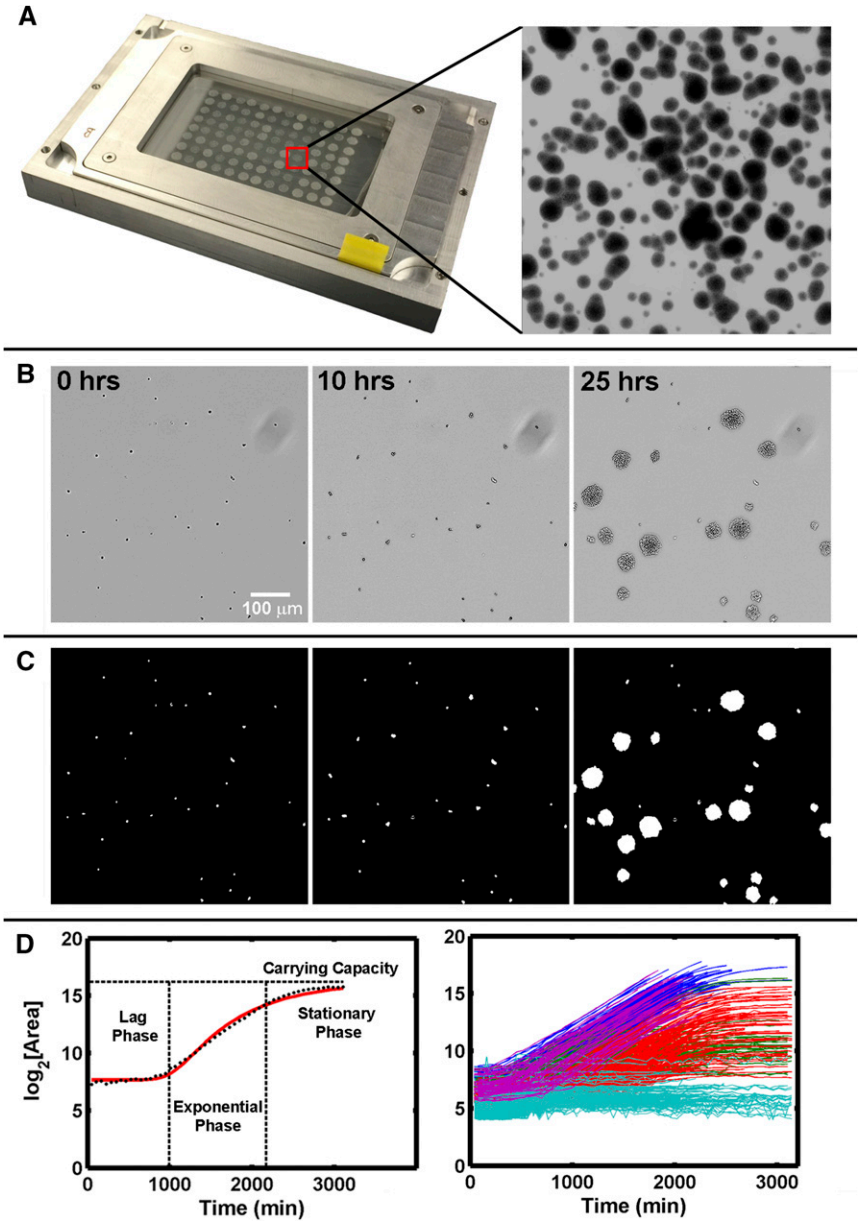

Figure 1 One-cell Doubling Evaluation by Living Arrays of Yeast (ODELAY). Solid-phase growth parameters are extracted by collecting time course image of growing colonies (A and B). Colony areas are measured from thresholded and binarized images from the time course image series (C). Colonies seeded from single yeast cells are tracked over time and the log2(Area) is used to fit a parameterized version of the Gompertz function (D, left). A control yeast strain (BY4741) was pregrown to saturation with glucose as a carbon source and then assayed on galactose-containing agar. The resulting heterogeneous colonies were clustered based on growth curve characteristics and graphed using colors to represent each cluster (D, right).

doubling times for 140 yeast strains correlated well between the two platforms with a Pearson coefficient of 0.76 and Spearman coefficient of 0.70 (Figure 2B). These correlation coefficients are similar to growth rate comparisons of growth on solid media versus liquid media reported elsewhere (Zackrisson *et al.* 2016). Growth rates measured with ODELAY correlate rather modestly with other colony pinned and liquid growth OD_{600} assays, which is also similarly reported (Zackrisson *et al.* 2016). These differences likely reflect differences in growth conditions employed in each experiment or method. ODELAY-derived lag times showed less agreement with liquid growth OD_{600} measurements, likely due to the liquid *vs.* solid culture medium, and the lack of sensitivity of optical density measurements at low cell concentrations (Figure 2B). In addition, unlike BioScreen, ODELAY identified slow growing outliers because microcolony growth curves are derived from single cells. In contrast, liquid culture OD_{600} curves measure an aggregate of all cells in a population, and therefore are not sensitive to the contribution of individual cells.

Microcolony convergence is the limiting factor of ODELAY's dynamic range, which can be controlled by altering the initial cell density obtained when spotting yeast cultures. Increased cell density decreases the time it takes for growing colonies to converge. In contrast, the dynamic range of liquid culture measurements is limited by either the nutrient capacity of the media or the linear range of the density sensor. Due to differences in strain doubling times, the dynamic range is best defined by the total number of doublings required to reach the upper limit starting from a single cell. At optimal seed density of ~200–500 cells per spot (~25–50 cells/mm^2), the dynamic range of ODELAY is 8–12 doublings, from a single cell up to 250 or as many as 4000 cells, which compares favorably to a dynamic range of 3–5 doublings attainable by most currently available technologies.

In traditional pinned colony assays, the size of a colony is dependent on the number of viable individuals contributing to the colony population, the number of doublings these cells have undergone, the amount of nutrients present, and the ability of the colony to transport nutrients to

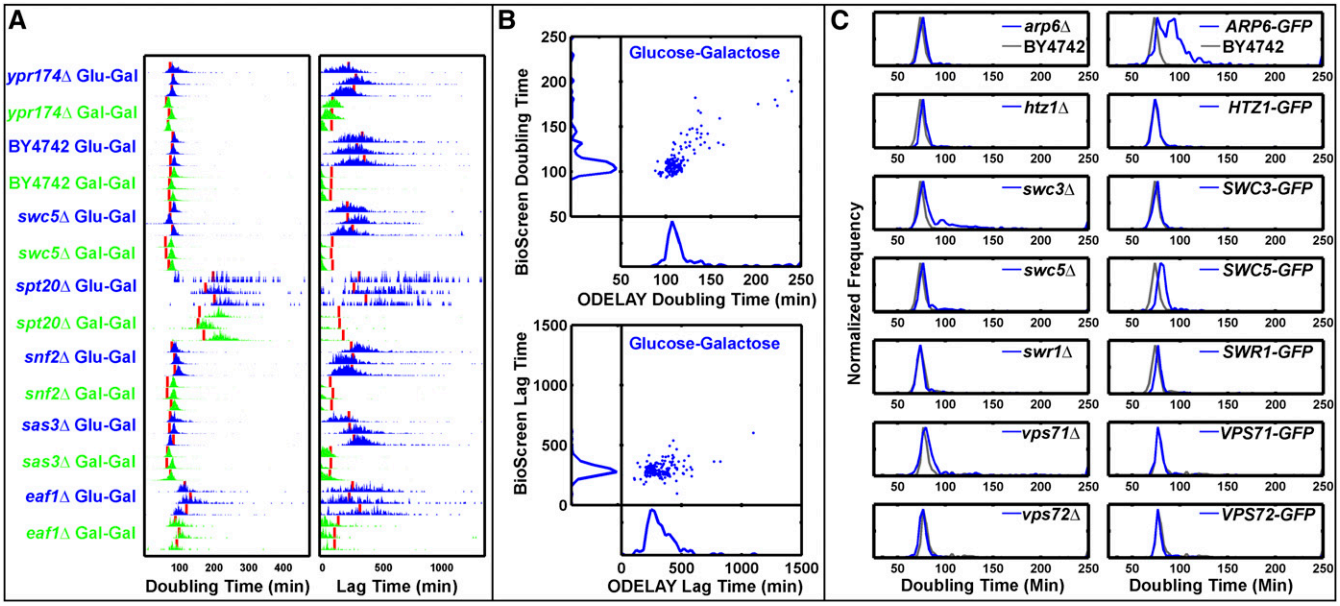

Figure 2 Complex phenotypes observed by ODELAY. Comparisons of doubling times and lag times for repeated measurements (A). Red lines indicate Bioscreen C results. Median ODELAY measurements show good agreement with BioScreen C measurements in doubling time but less so in lag time (B). Population histograms of doubling time from SWR1 complex deletion and GFP-tagged strains (blue) with comparison to the parent strain BY4742 (gray) (C). Heterogeneity in doubling times is observed in strains *swc3*Δ and *ARP6-GFP* while *arp6*Δ and *SWC3-GFP* appear similar to the parent strain BY4742. GFP, green fluorescent protein; ODELAY, One-cell Doubling Evaluation by Living Arrays of Yeast.

its reproducing members. The contribution of individuals to the overall colony size is not distinguished by traditional methods such as liquid-based or spot-based assays. In contrast, ODELAY tracks individual cells forming into colonies and can quantify population heterogeneity that other methods cannot resolve.

Example applications of ODELAY

Identification of doubling time phenotypes: To illustrate the ability of ODELAY to compare population heterogeneity of growth phenotypes between strains such that features of the population distributions may be evaluated, we focused on members of the SWR1 complex of chromatin modifiers (Figure 2C). Chromatin modification is one way for the emergence of epigenetic differences that can manifest as heterogeneity within isogenic populations. We observed population heterogeneity in two strains, *swc3*Δ and *ARP6-GFP* (Figure 2C), but not in their respective GFP-tagged or deletion mutant. Population heterogeneity has been observed before in SWR1 deletion strains when measuring *POT1-GFP* expression during a carbon source switch from glucose to oleic acid (Knijnenburg *et al.* 2011). In that instance, deletion of other members of the SWR1 deletion complex induced bimodal expression of *POT1-GFP*. Here, the bimodality of growth phenotypes emerged from cells grown strictly on glucose media and without any stimulation from a change in carbon source. This observation demonstrates that ODELAY readily detects subpopulations of cells present in standard culture of deletion and GFP fusion strains.

Identification of lag time phenotype: Through ODELAY analysis, outliers with highly variable, expanded, or contracted lag periods can be identified by assessing the distribution of lag times for microcolonies of a given strain (lag time variability), as well as relative lag between tested strains. To demonstrate the quantification of lag time by ODELAY, we exploited the well-studied and highly regulated response of yeast to a carbon source shift from its preferred source, glucose, to an alternative source, galactose (Guarente *et al.* 1982). This shift is characterized by a lag phase, during which the normally repressed galactose utilization machinery, including the galactose transporter, is induced. Exponentially growing yeast preconditioned in either glucose or galactose liquid medium were spotted onto solid media containing galactose and analyzed by ODELAY (Figure 4A). Cells preconditioned in galactose media exhibited a highly synchronized response characterized by short lag times. In contrast, more pronounced and variable lag times were observed for cells that were not primed for growth in galactose. Once glucose-grown cells acclimated to the shift to galactose and entered exponential phase, they doubled at rates similar to those observed for galactose preconditioned cells.

As with heterogeneity of doubling times, ODELAY enables the detection of heterogeneity in lag times. To demonstrate the utility of ODELAY in assessing population heterogeneity of lag times, we compared growth parameters of a control yeast strain (BY4742) in galactose-containing medium after pregrowth in glucose media for differing amounts of time (Figure 3A). We staggered seeding of cultures such that cells were pregrown in glucose media for 3, 6, 24, and 48 hr (Figure 3B). The resulting cultures were then spotted on galactose media and their growth phenotypes observed (Figure 3C). Not only did lag time correlate with the length of time that yeast was cultured in glucose but also colony-to-colony variation in lag times increased for the longer incubation times. This example demonstrates ODELAY's ability to capture the effects of environmental perturbations on population heterogeneity, a feature which is difficult to distinguish using other solid media growth assays.

Large-scale multiparameter analyses with ODELAY

A strength of the ODELAY platform is to extract doubling times and lag times for populations of cells growing on solid media in a high-throughput manner. To demonstrate multiparameter growth rate analysis by ODELAY, we assayed a collection of 140 strains that contained

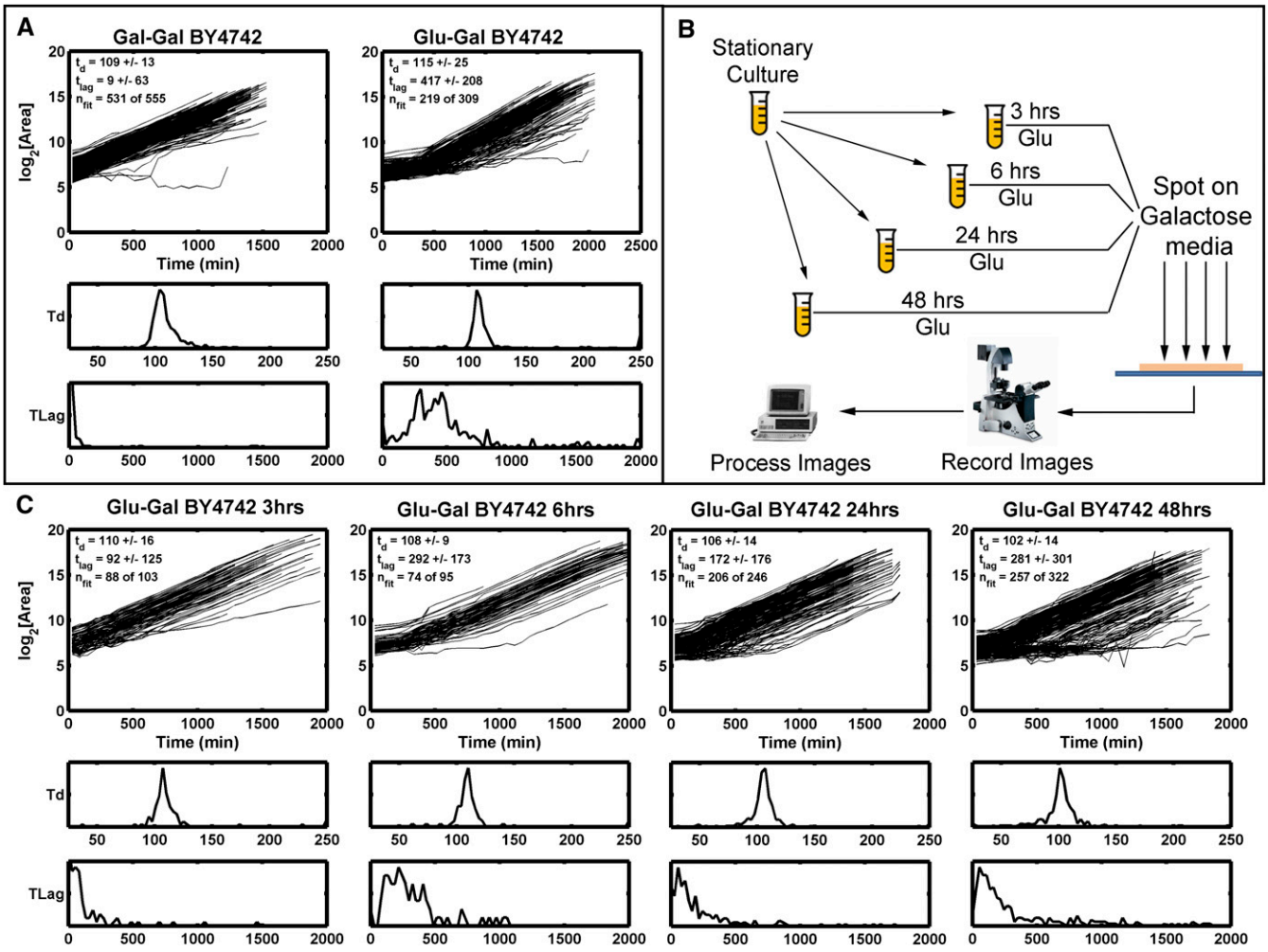

Figure 3 Observing lag time after a carbon source switch: Growth curves and histograms depicting lag time (TLag) and doubling time (Td) for control yeast strain (BY4742) pregrown in Gal (left) or Glu (right) and then spotted on Gal media (A). Differing growth phenotypes are observed from samples of a control yeast strain taken from the same culture at multiple times after seeding a source culture (B and C). Histograms of the Td and TLag are depicted below each set of growth curves. Note the changes in the lag time distributions as the source culture is aged. This demonstrates ODELAY's utility and sensitivity to culture conditions of yeast. Gal, galactose; Glu, glucose; ODELAY, One-cell Doubling Evaluation by Living Arrays of Yeast.

gene deletions of transcription factors, transcriptional regulators, and nuclear transport factors including nucleoporins and karyopherins. The genes selected were previously associated with regulating the response to a carbon source shift (Winzeler *et al.* 1999; Aitchison and Rout 2012; Knijnenburg *et al.* 2011; Van de Vosse *et al.* 2011).

For the deletion strains, we quantified colony doubling times and lag times, and estimated carrying capacities during a carbon source switch from glucose to galactose using galactose-to-galactose transition as a control. This rich multivariate dataset underscores how ODELAY can reveal complex and heterogeneous growth phenotypes of populations of individual cells growing into colonies (Figure 4). Strains with noticeably strong increases in doubling time include *dot1*Δ, *htl1*Δ, *eaf5*Δ, *eaf7*Δ, and *spt20*Δ. Of these five examples, only *spt20*Δ had been reported to have reduced growth rate on galactose media (Roberts and Winston 1996).

In general, reporting absolute values of growth parameters is rare in the literature. Here, we present a second large-scale application of ODELAY to compare doubling times of yeast mutants to the parent strain. A commonly overlooked class of mutant includes the C-terminal tagging with GFP, which is often assumed to have negligible effects on growth when compared with the more dramatic growth defects observed in deletion strains. We tested this assumption by comparing the doubling time of the previously mentioned deletion strains and the corresponding GFP fusion strains against their parent strain, BY4742. All measurements were repeated in triplicate on rich glucose media with the most frequently observed doubling time, the population mode, of each replicate compared to the parent strain using the Student's *t*-test. ODELAY was able to resolve 12 GFP fusions with doubling times significantly decreased compared to BY4742 and 71 strains that have significantly increased doubling times (Table 1). The deletion strains group had 11 strains with significantly decreased doubling times while 72 had significantly increased doubling times (Table 2). While the majority of the doubling time differences for the GFP strains were <5 min, the presence of the GFP tag does appear to have a widespread and significant impact on growth rates on rich media.

Comparison of ODELAY to other phenotypic analysis methods

ODELAY differs from colony pinning assays and liquid culture assays primarily in its ability to observe heterogeneity in lag time, doubling time, and carrying capacity of colonies forming from

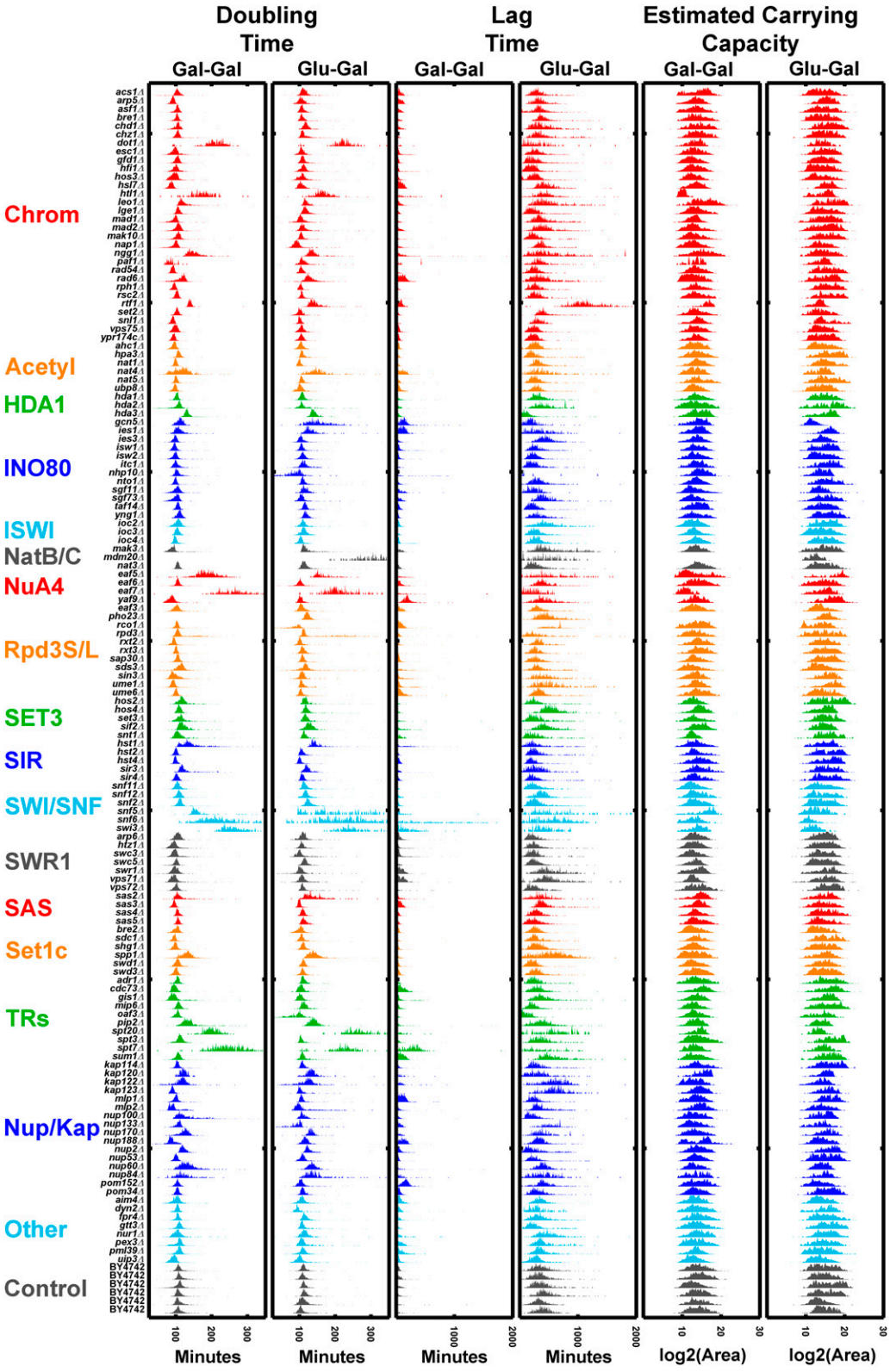

Figure 4 Comparison of 140 deletion strains: doubling times, lag times, and estimated carrying capacities of 140 deletion strains that underwent a Glu to Gal switch *vs.* those that were maintained on Gal as a carbon source. Strains are grouped into categories according to annotated gene function (yeastgenome.org) including chromatin modifiers (Chrom), acetyltransferase enzymes (Acetyl), protein complexes (HDA1, INO80, ISWI NatB/C, NuA4, Rpd3S/L, SET3, SIR, SWI/SNF, SWR1, SAS, and SetC), transcriptional regulators (TRs), nucleoporins and karyopherins (Nup/Kap), and other genes associated with carbon source switching (other). Gal, galactose; Glu, glucose.

individual cells. A summary of features of various growth assays are described (Table S2). While ODELAY is similar to previously published methods that observe colonies forming from single cells in liquid media (Levy *et al.* 2012), ODELAY is distinguished from these techniques by observing larger areas with image stitching and improved analysis of the resulting growth curves. In its current configuration, ODELAY can resolve individual cells with a pixel resolution of 0.65 μm and can evaluate 96 strains per assay. For each strain, up to 10^3 individual cells are observed growing into colonies with between 10^5 and 10^6 colonies observed per experiment. This

Table 1 GFP-tagged library mutants with significant growth difference over a control strain

Strain	Mean Doubling Time Increase	Doubling Time SD	*P*-Value
LGE1-GFP	−2.394	1.322	2.2E−07
KAP122-GFP	−1.158	2.177	8.3E−45
GCN5-GFP	−0.922	0.660	5.9E−18
EAF7-GFP	−0.829	2.023	1.4E−50
HDA2-GFP	−0.724	1.110	3.1E−24
KAP123-GFP	−0.666	0.633	3.1E−02
ACS1-GFP	−0.393	0.952	1.3E−02
RAD54-GFP	−0.334	0.576	1.1E−03
NGG1-GFP	−0.298	1.134	1.5E−45
YPR174c-GFP	−0.231	1.496	3.1E−02
DYN2-GFP	−0.175	0.307	1.1E−02
HOS2-GFP	−0.060	0.848	2.2E−02
LEO1-GFP	0.010	0.323	3.7E−18
ASF1-GFP	0.099	0.362	7.5E−05
RXT3-GFP	0.160	1.441	2.3E−03
NUP84-GFP	0.246	0.427	1.9E−52
RCO1-GFP	0.325	0.301	1.1E−03
NUP100-GFP	0.339	0.248	1.3E−36
PEX3-GFP	0.405	0.743	3.9E−02
SAS4-GFP	0.413	1.987	4.3E−02
NUP2-GFP	0.441	0.114	4.6E−18
SPT7-GFP	0.532	1.758	1.5E−61
ISW1-GFP	0.553	1.250	2.2E−02
PIP2-GFP	0.587	0.596	7.2E−24
NAT4-GFP	0.653	1.637	2.6E−53
KAP120-GFP	0.668	1.158	4.0E−31
MAK3-GFP	0.683	1.510	1.6E−07
SUM1-GFP	0.725	0.267	1.0E−02
ITC1-GFP	0.764	0.945	4.0E−10
NHP10-GFP	0.806	1.058	4.6E−02
SNL1-GFP	0.942	1.119	8.5E−17
SPP1-GFP	0.949	1.110	2.4E−16
NUP60-GFP	0.961	1.293	9.7E−08
SWR1-GFP	0.972	1.490	1.1E−03
SIR3-GFP	1.004	1.528	2.3E−22
HOS3-GFP	1.039	0.958	1.1E−03
NAT5-GFP	1.094	1.526	1.4E−04
GFD1-GFP	1.200	0.646	2.1E−03
SGF73-GFP	1.268	1.078	7.6E−03
HOS4-GFP	1.271	0.860	1.2E−05
DOT1-GFP	1.276	1.004	5.5E−69
SWC3-GFP	1.303	0.889	1.5E−15
UME1-GFP	1.380	1.055	1.2E−66
IES1-GFP	1.381	0.290	7.5E−24
HDA3-GFP	1.584	0.597	5.3E−49
AIM4-GFP	1.585	0.655	4.1E−02
HST1-GFP	1.615	1.890	4.5E−50
NUP53-GFP	1.623	2.957	1.7E−10
SWI3-GFP	1.663	1.046	4.2E−80
UBP8-GFP	1.681	0.419	2.4E−02
IES3-GFP	1.793	1.606	1.5E−15
SNT1-GFP	1.804	0.636	1.6E−12
IOC2-GFP	1.883	0.652	1.0E−04
SET3-GFP	2.004	1.511	9.7E−16
CHZ1-GFP	2.006	0.959	7.2E−09
NUP170-GFP	2.062	0.738	2.0E−08
HTL1-GFP	2.063	1.546	9.1E−54
SNF2-GFP	2.091	1.500	1.8E−17
SPT20-GFP	2.276	1.150	3.4E−99
BRE2-GFP	2.311	1.719	3.7E−02
SWC5-GFP	2.344	1.867	2.8E−02
VPS71-GFP	2.376	2.383	5.7E−04
NUP133-GFP	2.421	1.157	3.7E−03
EAF5-GFP	2.532	1.120	4.0E−66
NTO1-GFP	2.548	2.321	9.6E−04
RTF1-GFP	2.629	1.378	6.2E−25
YNG1-GFP	2.768	1.554	3.2E−02
RAD6-GFP	2.882	1.944	3.6E−26
NUP188-GFP	2.884	1.108	6.2E−04
PHO23-GFP	2.919	1.251	2.4E−08
SDS3-GFP	2.920	2.550	1.9E−02
SWD3-GFP	3.017	2.390	5.9E−03
TAF14-GFP	3.058	1.181	4.8E−02
SIF2-GFP	3.255	0.989	2.3E−04
PAF1-GFP	3.321	0.627	2.2E−11
SNF5-GFP	3.384	3.158	1.6E−30
SAP30-GFP	3.482	2.152	3.0E−03
SAS2-GFP	3.518	1.641	5.5E−42
SNF12-GFP	4.084	0.709	1.5E−07
MDM20-GFP	4.545	1.486	1.9E−92
CDC73-GFP	5.254	1.304	3.9E−05
SNF6-GFP	5.270	0.543	1.5E−60
RPD3-GFP	11.697	0.679	1.2E−22

GFP, green fluorescent protein.

feature allows clear observation of population heterogeneity, to which most other methods are insensitive, and allows new avenues for characterizing variations cellular growth phenotypes, even for well-studied organisms such as baker's yeast.

Periodically imaged colony pinning assays, such as ultrahigh-density omics (Bean *et al.* 2014), Scan-o-matic (Zackrisson *et al.* 2016), and ScanLag (Levin-Reisman *et al.* 2010), have very high throughput in terms observing from 96 to 6144 colonies per plate, with 1536 colonies being typical (Table S2). Each colony has the potential to be a unique strain, allowing complete screening of yeast libraries within a short period of time. However, arraying colonies at higher densities limits the total observation time from when a colony can be clearly resolved by the imaging methods to when the colonies merge (Bean *et al.* 2014). Herein lies the tradeoff between ODELAY and pinned assays; ODELAY may observe heterogeneity at the cost of total number of strains observed. Though it should be noted that, as with colony pinning assays, ODLEAY's strain throughput can be increased with improved tooling.

Similar to other growth assays, there are caveats associated with ODELAY. Extraction of cell doubling time by ODELAY relies on the assumption that microcolony cross-sectional area is directly proportional to the volume of cells in a given colony and that this relationship between volume and area is unaffected by changes in growth condition and/or genetic background. There will certainly be exceptions to this assumption in yeast and other colony forming micro-organisms; however, similar to the limitations in liquid culture OD_{600} analysis when applied to flocculent mutant strains, such exceptions may yield informative phenotypic information. Furthermore, ODELAY could be adapted to analyze the 3D volume of the growing microcolonies; however, this would trade off time for collecting images or limit the total area interrogated. Lag time measurements were also observed to have local variations, which are also commonly observed in other solid phase growth assays

Table 2 Deletion library strains with significant difference in doubling time over control strain

Strain	Mean Doubling Time Increase	Doubling Time SD	*P*-Value
snl1Δ	−7.92	0.16	8.4E−17
cdc73Δ	−3.41	1.26	3.9E−05
asf1Δ	−3.34	2.19	7.4E−05
nat5Δ	−3.14	1.35	1.4E−04
rad54Δ	−2.65	0.99	1.1E−03
swr1Δ	−2.65	0.12	1.0E−03
rxt3Δ	−2.46	0.67	2.3E−03
dyn2Δ	−2.04	0.80	1.1E−02
acs1Δ	−2.02	1.66	1.3E−02
ksp123Δ	−1.72	0.39	3.0E−02
sas4Δ	−1.61	0.45	4.2E−02
swc5Δ	0.97	1.91	2.7E−02
ypr174Δc	1.03	1.32	3.1E−02
yng1Δ	1.56	6.11	3.2E−02
nhp10Δ	1.59	0.57	4.6E−02
taf14Δ	1.59	1.24	4.7E−02
pex3Δ	1.66	1.21	3.8E−02
aim4Δ	1.67	2.16	4.0E−02
bre2Δ	1.68	1.48	3.7E−02
ubp8Δ	1.80	0.34	2.4E−02
hos2Δ	1.83	0.72	2.2E−02
isw1Δ	1.83	0.66	2.1E−02
sds3Δ	1.87	0.52	1.9E−02
sum1Δ	2.11	2.09	1.0E−02
sgf73Δ	2.21	2.44	7.5E−03
swd3Δ	2.33	3.05	5.8E−03
nup133Δ	2.34	0.62	3.6E−03
sap30Δ	2.42	1.62	3.0E−03
gfd1Δ	2.49	0.40	2.0E−03
nto1Δ	2.69	0.95	9.6E−04
hos3Δ	2.69	1.99	1.1E−03
rco1Δ	2.71	2.09	1.0E−03
nup188Δ	2.79	0.89	6.2E−04
vps71Δ	2.87	2.14	5.6E−04
Sif2Δ	3.04	1.50	2.2E−04
loc2Δ	3.22	1.36	1.0E−04
hos4Δ	3.69	1.73	1.1E−05
snf2Δ	4.19	2.18	1.8E−17
spp1Δ	4.41	2.31	2.3E−16
lge1Δ	4.42	1.17	2.1E−07
mak3Δ	4.46	0.94	1.6E−07
snf12Δ	4.49	1.34	1.4E−07
nup60Δ	4.53	0.58	9.7E−08
nup170Δ	4.81	0.49	2.0E−08
pho23Δ	4.83	1.46	2.3E−08
chz1Δ	5.06	1.67	7.1E−09
itc1Δ	5.49	0.87	3.9E−10
paf1Δ	5.97	0.90	2.2E−11
snt1Δ	6.59	2.49	1.5E−12
asm4Δ	6.94	8.51	1.6E−10
set3Δ	7.55	0.52	9.7E−16
ies3Δ	7.57	1.53	1.5E−15
swc3Δ	7.82	2.89	1.5E−15
nup2Δ	8.41	0.77	4.5E−18
leo1Δ	8.45	0.85	3.7E−18
gcn5Δ	8.47	1.63	5.9E−18
sir3Δ	9.99	0.36	2.2E−22
rpd3Δ	10.20	1.39	1.1E−22
pip2Δ	10.58	0.76	7.2E−24
ies1Δ	11.08	3.03	7.5E−24
hda2Δ	11.16	2.81	3.0E−24
rtf1Δ	11.52	3.02	6.2E−25
rad6Δ	11.96	2.83	3.5E−26
kap120Δ	13.76	1.97	3.9E−31
nup10Δ	16.68	2.95	1.2E−36
sas2Δ	20.44	4.35	5.5E−42
ngg1Δ	21.17	2.52	1.4E−45
kap122Δ	22.07	4.32	8.3E−45
hda3Δ	22.77	1.66	5.3E−49
hst1Δ	23.95	2.62	4.5E−50
nup84Δ	24.82	1.41	1.8E−52
htl1Δ	25.90	1.86	9.1E−54
nat4Δ	26.32	2.95	2.5E−53
eaf5Δ	28.32	6.34	4.0E−66
spt7Δ	36.15	5.62	1.5E−61
ume1Δ	39.04	4.49	1.2E−66
eaf7Δ	41.02	13.45	1.4E−50
dot1Δ	41.67	4.65	5.4E−69
swi3Δ	54.40	4.50	4.1E−80
spt20Δ	73.09	8.36	3.4E−99
snf6Δ	85.92	24.82	1.4E−60
snf5Δ	101.28	70.92	1.6E−30
mdm20Δ	101.37	10.87	1.9E−92

(Baryshnikova *et al.* 2010; Levin-Reisman *et al.* 2010). Although all initial experiments have utilized haploid baker's yeast, this methodology can be applied in other colony-forming organisms including medically relevant bacteria such as *Mycobacterium tuberculosis*, *Pseudomonas aeruginosa*, *Staphylococcus aureus*, and others.

In summary, ODELAY is a quantitative tool capable of multiparameter growth analysis based on time resolved microcolony expansion on solid media. The unique features of ODELAY include its relatively large dynamic range, when compared to other available methods, which enables quantitative measurement of doubling time, lag time, and carrying capacity in a single experiment. Additionally, ODELAY has the ability to assess population heterogeneity, including viability, through the analysis of single microcolonies.

ACKNOWLEDGMENTS

We thank the Luxembourg Centre for Systems Biomedicine and the University of Luxembourg for support. In addition, we thank A. Blomberg and M. Zackrisson for sharing data for Figure S1. The authors acknowledge support for this work by grants U54 RR022220, P41 GM109824, R01 GM112108 and P50 GM076547 to J.D.A. from the US National Institutes of Health.

Author contributions: D.J.D. conceived the ODELAY method; ODELAY was developed by T.H., A.V.R., and D.J.D., with intellectual support from S.L., F.D.M., J.J.S., and J.D.A.; T.H. and S.L. performed all experiments; T.H. and D.J.D. wrote the manuscript with contributions from A.V.R., F.D.M., J.J.S., and J.D.A.

LITERATURE CITED

Aitchison, J. D., and M. P. Rout, 2012 The yeast nuclear pore complex and transport through it. Genetics 190: 855–883.

Baryshnikova, A., M. Costanzo, Y. Kim, H. Ding, J. Koh *et al.*, 2010 Quantitative analysis of fitness and genetic interactions in yeast on a genome scale. Nat. Methods 7: 1017–1024.

Bean, G. J., P. A. Jaeger, S. Bahr, and T. Ideker, 2014 Development of ultra-high-density screening tools for microbial "omics." PLoS One 9: e85177.
Breslow, D. K., D. M. Cameron, S. R. Collins, M. Schuldiner, J. Stewart-Ornstein *et al.*, 2008 A comprehensive strategy enabling high-resolution functional analysis of the yeast genome. Nat. Methods 5: 711–718.
Bryan, A. K., A. Goranov, A. Amon, and S. R. Manalis, 2010 Measurement of mass, density, and volume during the cell cycle of yeast. Proc. Natl. Acad. Sci. USA 107: 999–1004.
Collins, S. R., M. Schuldiner, N. J. Krogan, and J. S. Weissman, 2006 A strategy for extracting and analyzing large-scale quantitative epistatic interaction data. Genome Biol. 7: R63.
Costanzo, M., A. Baryshnikova, J. Bellay, Y. Kim, E. D. Spear *et al.*, 2010 The genetic landscape of a cell. Science 327: 425–431.
Costanzo, M., B. VanderSluis, E. N. Koch, A. Baryshnikova, C. Pons *et al.*, 2016 A global genetic interaction network maps a wiring diagram of cellular function. Science DOI: 10.1126/science.aaf1420.
Deutschbauer, A. M., D. F. Jaramillo, M. Proctor, J. Kumm, M. E. Hillenmeyer *et al.*, 2005 Mechanisms of haploinsufficiency revealed by genome-wide profiling in yeast. Genetics 169: 1915–1925.
Edelstein, A. D., M. A. Tsuchida, N. Amodaj, H. Pinkard, R. D. Vale *et al.*, 2014 Advanced methods of microscope control using μManager software. J. Biol. Methods 1: 10.
Godin, M., F. F. Delgado, S. Son, W. H. Grover, A. K. Bryan *et al.*, 2010 Using buoyant mass to measure the growth of single cells. Nat. Methods 7: 387–390.
Gompertz, B., 1825 On the nature of the function expressive of the law of human mortality, and on a new mode of determining the value of life contingencies. Philos. Trans. R. Soc. Lond. 115: 513–583.
Guarente, L., R. R. Yocum, and P. Gifford, 1982 A GAL10–CYC1 hybrid yeast promoter identifies the GAL4 regulatory region as an upstream site. Proc. Natl. Acad. Sci. USA 79: 7410–7414.
Jørgensen, H. L., and E. Schulz, 1985 Turbidimetric measurement as a rapid method for the determination of the bacteriological quality of minced meat. Int. J. Food Microbiol. 2: 177–183.
Knijnenburg, T. A., O. Roda, Y. Wan, G. P. Nolan, J. D. Aitchison *et al.*, 2011 A regression model approach to enable cell morphology correction in high-throughput flow cytometry. Mol. Syst. Biol. 7: 531.
Kortmann, H., L. M. Blank, and A. Schmid, 2009 Single cell analysis reveals unexpected growth phenotype of S. cerevisiae. Cytom. Part J. Int. Soc. Anal. Cytol. 75: 130–139.
Lawless, C., D. J. Wilkinson, A. Young, S. G. Addinall, and D. A. Lydall, 2010 Colonyzer: automated quantification of micro-organism growth characteristics on solid agar. BMC Bioinformatics 11: 287.
Levin-Reisman, I., O. Gefen, O. Fridman, I. Ronin, D. Shwa *et al.*, 2010 Automated imaging with ScanLag reveals previously undetectable bacterial growth phenotypes. Nat. Methods 7: 737–739.
Levy, S. F., N. Ziv, and M. L. Siegal, 2012 Bet hedging in yeast by heterogeneous, age-correlated expression of a stress protectant. PLoS Biol. 10: e1001325.
Memarian, N., M. Jessulat, J. Alirezaie, N. Mir-Rashed, J. Xu *et al.*, 2007 Colony size measurement of the yeast gene deletion strains for functional genomics. BMC Bioinformatics 8: 117.
Monod, J., 1949 The growth of bacterial cultures. Annu. Rev. Microbiol. 3: 371–394.
Murakami, C., and M. Kaeberlein, 2009 Quantifying yeast chronological life span by outgrowth of aged cells. J. Vis. Exp. 27: e1156.
Pertuz, S., D. Puig, and M. A. Garcia, 2013 Analysis of focus measure operators for shape-from-focus. Pattern Recognit. 46: 1415–1432.
Peskett, G. L., 1927 Studies on the growth of yeast: a nephelometric method of counting yeast suspensions. Biochem. J. 21: 460–466.
Preibisch, S., S. Saalfeld, and P. Tomancak, 2009 Globally optimal stitching of tiled 3D microscopic image acquisitions. Bioinformatics 25: 1463–1465.
Roberts, S. M., and F. Winston, 1996 SPT20/ADA5 encodes a novel protein functionally related to the TATA-binding protein and important for transcription in Saccharomyces cerevisiae. Mol. Cell. Biol. 16: 3206–3213.
Shah, N. A., R. J. Laws, B. Wardman, L. P. Zhao, and J. L. Hartman, 2007 Accurate, precise modeling of cell proliferation kinetics from time-lapse imaging and automated image analysis of agar yeast culture arrays. BMC Syst. Biol. 1: 3.
Sun, J., C. C. Stowers, E. M. Boczko, and D. Li, 2010 Measurement of the volume growth rate of single budding yeast with the MOSFET-based microfluidic Coulter counter. Lab Chip 10: 2986–2993.
Tucker, C. L., and S. Fields, 2004 Quantitative genome-wide analysis of yeast deletion strain sensitivities to oxidative and chemical stress. Comp. Funct. Genomics 5: 216–224.
Van de Vosse, D. W., Y. Wan, R. W. Wozniak, and J. D. Aitchison, 2011 Role of the nuclear envelope in genome organization and gene expression. Wiley Interdiscip. Rev. Syst. Biol. Med. 3: 147–166.
Warringer, J., D. Anevski, B. Liu, and A. Blomberg, 2008 Chemogenetic fingerprinting by analysis of cellular growth dynamics. BMC Chem. Biol. 8: 3.
Winzeler, E. A., D. D. Shoemaker, A. Astromoff, H. Liang, K. Anderson *et al.*, 1999 Functional characterization of the S. cerevisiae genome by gene deletion and parallel analysis. Science 285: 901–906.
Yoshikawa, K., T. Tanaka, C. Furusawa, K. Nagahisa, T. Hirasawa *et al.*, 2009 Comprehensive phenotypic analysis for identification of genes affecting growth under ethanol stress in Saccharomyces cerevisiae. FEMS Yeast Res. 9: 32–44.
Zackrisson, M., J. Hallin, L.-G. Ottosson, P. Dahl, E. Fernandez-Parada *et al.*, 2016 Scan-o-matic: high-resolution microbial phenomics at a massive scale. G3 6: 3003–3014.
Zwietering, M. H., I. Jongenburger, F. M. Rombouts, and K. van 't Riet, 1990 Modeling of the bacterial growth curve. Appl. Environ. Microbiol. 56: 1875–1881.

Communicating editor: C. Nislow